

# Comet 67P/Churyumov–Gerasimenko preserved the pebbles that formed planetesimals

Marco Fulle,<sup>1★</sup> V. Della Corte,<sup>2</sup> A. Rotundi,<sup>2,3★</sup> F. J. M. Rietmeijer,<sup>4★</sup> S. F. Green,<sup>5</sup> P. Weissman,<sup>6</sup> M. Accolla,<sup>7</sup> L. Colangeli,<sup>8</sup> M. Ferrari,<sup>2</sup> S. Ivanovski,<sup>2</sup> J. J. Lopez-Moreno,<sup>9</sup> E. Mazzotta Epifani,<sup>10</sup> R. Morales,<sup>9</sup> J. L. Ortiz,<sup>9</sup> E. Palomba,<sup>2</sup> P. Palumbo,<sup>3,2</sup> J. Rodriguez,<sup>9</sup> R. Sordini<sup>2</sup> and V. Zakharov<sup>11,12</sup>

<sup>1</sup>INAF – Osservatorio Astronomico, Via Tiepolo 11, I-34143 Trieste, Italy

<sup>2</sup>INAF – Istituto di Astrofisica e Planetologia Spaziali, Via Fosso del Cavaliere 100, I-00133 Rome, Italy

<sup>3</sup>Università degli Studi di Napoli Parthenope, Dip. di Scienze e Tecnologie, CDN IC4, I-80143 Naples, Italy

<sup>4</sup>Department of Earth and Planetary Sciences, MSC03 2040, 1-University of New Mexico, Albuquerque, NM 87131-0001, USA

<sup>5</sup>Planetary and Space Sciences, Department of Physical Sciences, The Open University, Milton Keynes MK7 6AA, UK

<sup>6</sup>Planetary Science Institute, 1700 East Fort Lowell, Suite 106, Tucson, AZ 85719, USA

<sup>7</sup>INAF – Osservatorio Astronomico di Catania, via S. Sofia 78, I-95123 Catania, Italy

<sup>8</sup>ESA - ESTEC, European Space Agency, Keplerlaan 1, NL-2201 AZ Noordwijk, the Netherlands

<sup>9</sup>Instituto de Astrofísica de Andalucía (CSIC), Glorieta de la Astronomía s/n, E-18008 Granada, Spain

<sup>10</sup>INAF – Osservatorio Astronomico di Roma, Via di Frascati 33, Monte Porzio Catone, Rome, Italy

<sup>11</sup>LESIA-Observatoire de Paris, CNRS, UPMC, Université Paris-Diderot, 5 place Jules Janssen, F-92195 Meudon, France

<sup>12</sup>Sorbonne Universités, UPMC Univ Paris 06, CNRS, Laboratoire de Meteorologie Dynamique, 4 place Jussieu, F-75252 Paris, France

Accepted 2016 September 9. Received 2016 September 6; in original form 2016 July 8

## ABSTRACT

Solar system formation models predict that the building blocks of planetesimals were mm- to cm-sized pebbles, aggregates of ices and non-volatile materials, consistent with the compact particles ejected by comet 67P/Churyumov–Gerasimenko (67P hereafter) and detected by GIADA (Grain Impact Analyzer and Dust Accumulator) on-board the Rosetta spacecraft. Planetesimals were formed by the gentle gravitational accretion of pebbles, so that they have an internal macroporosity of 40 per cent. We measure the average dust bulk density  $\rho_D = 795^{+840}_{-65}$  kg m<sup>-3</sup> that, coupled to the nucleus bulk density, provides the average dust-to-ices mass ratio  $\delta = 8.5$ . We find that the measured densities of the 67P pebbles are consistent with a mixture of  $(15 \pm 6)$  per cent of ices,  $(5 \pm 2)$  per cent of Fe-sulphides,  $(28 \pm 5)$  per cent of silicates, and  $(52 \pm 12)$  per cent of hydrocarbons, in average volume abundances. This composition matches both the solar and CI-chondritic chemical abundances, thus showing that GIADA has sampled the typical non-volatile composition of the pebbles that formed all planetesimals. The GIADA data do not constrain the abundance of amorphous silicates versus crystalline Mg, Fe-olivines and pyroxenes. We find that the pebbles have a microporosity of  $(52 \pm 8)$  per cent (internal volume filling factor  $\phi_P = 0.48 \pm 0.08$ ), implying an average porosity for the 67P nucleus of  $(71 \pm 8)$  per cent, lower than previously estimated.

**Key words:** space vehicles – comets: general – comets: individual: 67P/Churyumov–Gerasimenko.

## 1 INTRODUCTION

According to models of the proto-planetary nebula (Lambrechts & Johansen 2012), gas streaming instabilities (Youdin & Goodman

2005; Johansen et al. 2007) will concentrate pebbles (Zsom et al. 2010; Wahlberg Jansson & Johansen 2014) into clouds that form planetesimals by gentle gravitational collapse. This is the most direct and simple way to overcome the so-called bouncing barrier (Zsom et al. 2010), above which mutual collisions destroy the pebbles, thereby stopping any further growth by pebble sticking into forming embryonic planetesimals. Wahlberg Jansson & Johansen (2014) show that gas streaming instabilities can explain the

\* E-mail: fulle@oats.inaf.it (MF); rotundi@uniparthenope.it (AR); fransjmr@unm.edu (FJMR)

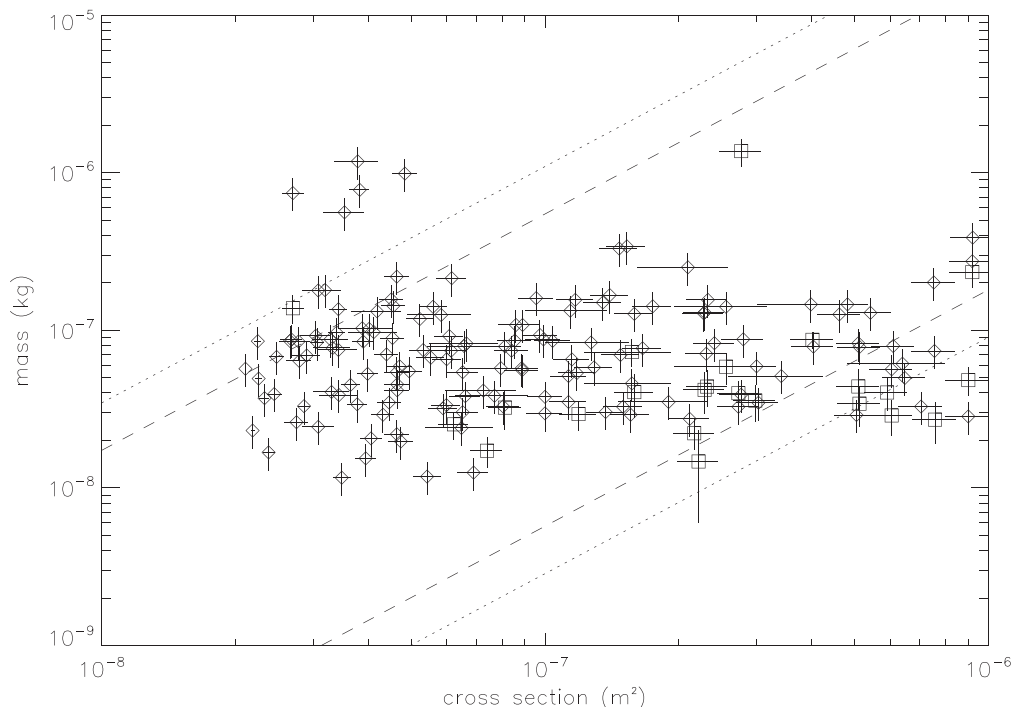


**Figure 1.** Mass and cross-section  $\chi$  measurements of compact particles detected by GIADA from 2014 August to 2016 April (diamonds and squares, the error bars refer to  $1 - \sigma$  standard error of the 167 measurements). Squares: 22 detections of compact particles occurred at the beginning of the GIADA dust showers of fluffy particles. The data are compared with the trends of prolate and oblate ellipsoids of aspect ratio of ten (dotted lines) and five (dashed lines) and with dust bulk densities of Fe-sulphides,  $\rho_1 = 4600 \text{ kg m}^{-3}$  (upper lines), and of hydrocarbons,  $\rho_3 = 1200 \text{ kg m}^{-3}$  (lower lines). Particles located between the upper lines may have a larger content of e.g. magnetite, with a higher bulk density than Fe-sulphides; those between and below the lower lines have a high porosity. The GDS signal saturates at  $\chi > 10^{-6} \text{ m}^2$ . Particles with mass  $< 10^{-8} \text{ kg}$  or  $\chi < 2 \times 10^{-8} \text{ m}^2$  were too small and fast to be detected by GDS. The flux at masses  $> 2 \times 10^{-7} \text{ kg}$  was very low during the entire mission due to the spacecraft safety constraints.

birth of planetesimals as small as comets. These models depend on the chemical and physical properties of the pebbles (Zsom et al. 2010; Wahlberg Jansson & Johansen 2014) that can be constrained by the properties of dust ejected from the 67P nucleus (Rotundi et al. 2015; Fulle et al. 2015). An important parameter constraining 67P origin is the pebble microporosity, which can be extracted from the GIADA dust data coupled to the average bulk density of the 67P nucleus (Pätzold et al. 2016). The average porosity of the 67P nucleus is provided by the pebble microporosity, and by the planetesimal macroporosity of 40 per cent, according to models of random packing of spheres (Onoda & Liniger 1990; Song, Wang & Makse 2008).

Davidsson et al. (2016) have shown that most Rosetta data are inconsistent with a collision-driven origin of this Jupiter Family Comet (Farinella & Davies 1996). According to Davidsson et al. (2016), 67P is a primordial rubble pile of metre-sized building-blocks, which has never experienced collisions at speeds larger than a few tens of  $\text{m s}^{-1}$  in the scattered disc, so that it cannot be a fragment of a much larger body (Davidsson et al. 2016). The material of 67P has never been significantly heated either by collisions or by the decay of radionuclides (Davidsson et al. 2016), thanks to a probable late accretion (Wahlberg Jansson & Johansen 2014). These evidences can be translated into a set of linear equations describing the internal structure of comets, with solutions (i.e. the mineralogy and porosity of the pebbles) that are all constrained by the Rosetta mission. To reach this goal, the ‘missing tile’ is provided by GIADA, which measures the dust bulk densities. These densities demonstrate that the 67P mineralogy is consistent with the elemental abundances of the pristine materials measured in our

Solar system. In this paper, we define as ‘pebbles’ the building blocks of 67P, which may have a typical size ranging from some millimetres (Johansen et al. 2007) to some metres (Davidsson et al. 2016).

## 2 GIADA DATA

GIADA measures the speed, scattered light, and the momentum of individual dust particles by means of two subsystems (Della Corte et al. 2014): a laser curtain plus photodiodes (GDS, grain detection system) and a plate connected to piezoelectric sensors (IS, impact sensor). Coupled GDS+IS detections provide the mass of the compact particles and, by calibrations performed on GIADA with cometary dust analogues (Ferrari et al. 2014), their geometrical cross-section (Della Corte et al. 2015, 2016). The analogues (carbons, olivines, pyroxenes, and sulphides) were selected to represent the dominant constituents in primitive extraterrestrial materials. Their shape is often far from spheres (Ferrari et al. 2014), and is here approximated by ellipsoids. Fig. 1 shows mass versus cross-section  $\chi$  measured for compact particles detected from 2014 August to 2016 April. The lines enveloping most GIADA data (Fig. 1) refer to the dust bulk densities of Fe-sulphides,  $\rho_1 = 4600 \text{ kg m}^{-3}$ , and of hydrocarbons,  $\rho_3 = 1200 \text{ kg m}^{-3}$ . The upper lines refer to prolate ellipsoids of mass  $\frac{4}{3} k \rho_1 \sqrt{\chi^3/\pi}$ , and the lower lines to oblate ellipsoids of mass  $\frac{4}{3} k^{-1} \rho_3 \sqrt{\chi^3/\pi}$ , both with aspect ratios of  $k = 5$  and  $k = 10$ . Most bulk densities fall within these two extremes, and cannot be better constrained because they are convolved with the actual shape, composition, and microporosity of each particle. Five

data points plotting at the upper-left in Fig. 1 are probably due to GDS spurious signals (Della Corte et al. 2016). Assuming a size-independent dust bulk density in the pebbles, the data in Fig. 1 provide the weighted average dust bulk density  $\rho_D = 795^{+840}_{-65} \text{ kg m}^{-3}$ , where the weights are the inverse of the bulk density error derived from each error pair in Fig. 1. The assumed average shape is spherical, i.e. consistent with the symmetric oblate and prolate ellipsoids enveloping all the data. The standard deviation was computed taking into account the shape (assumed  $k \leq 10$ ), that is the main source of data dispersion in Fig. 1.

The squares in Fig. 1 refer to compact particles that occurred at the beginning of the GDS-only dust showers (a second class of GIADA particles), which are the products of fragmentation, by the internal electrostatic tension, of fluffy dust aggregates (parents) charged by the secondary electron flux from Rosetta (Fulle et al. 2015). The fragments are decelerated to speeds of a few  $\text{cm s}^{-1}$  by the Rosetta electric field, so that their kinetic energy is that observed by RPC/IES (Rosetta Plasma Consortium Ion Electron Sensor) in some electron bursts of 0.2–20 keV (Burch et al. 2015). The predicted fractal dimension of the fragments is 1.87 (Fulle et al. 2015), which implies a low volume filling factor in the dust observed in the showers,  $\phi_F < 10^{-3}$ . Fluffy parent particles account for  $\approx 15$  per cent of the total non-volatile volume, but for  $< 1$  per cent of the total non-volatile mass (Fulle et al. 2015). Most squares fall to the right in Fig. 1, suggesting a compact seed embedded in a fluffy envelope, which lowers the average bulk density.

### 3 A MODEL OF PLANETESIMALS

We assume that the 67P nucleus is representative of a primitive planetesimal, i.e. that its structure and composition is homogeneous from a depth of a metre downwards. This assumption is supported by the results of RSI (Radio Science Investigation), excluding inhomogeneities at scales larger than hundreds metres (Pätzold et al. 2016), and of CONSERT (Comet Nucleus Sounding Experiment by Radio Transmission), excluding inhomogeneities at scales larger than ten metres (Kofman et al. 2015). The erosion of many metres in the southern hemi-nucleus at perihelion, and the airfall of a significant fraction of this material on the northern hemi-nucleus (Keller et al. 2015), allow us to assume that GIADA has sampled the typical non-volatile component of 67P. Classical rubble piles fit this scenario: the model we propose is actually independent of the pebble size, which may range from millimetres, according to formation models of planetesimals based on a gentle gravitational accretion of pebbles due to gas flow instabilities (Youdin & Goodman 2005; Johansen et al. 2007), up to some metres in case of primordial rubble piles (Davidsson et al. 2016). The results of this model allow us to further exclude a collision-driven origin of 67P, and to constrain the upper limit of collision speeds experienced by 67P.

About 10- $\mu\text{m}$ -sized grains of Fe-sulphide and Mg-olivine were present among the particles collected at comet 81P/Wild 2 (Brownlee et al. 2006), and among non-chondritic cometary particles collected in the Earth's atmosphere (Zolensky & Thomas 1995; Rietmeijer et al. 2002). The lack of  $\text{Fe}_2^+$  bands in the 67P IR spectra (Capaccioni et al. 2015) and the 81P/Wild 2 olivine and pyroxene compositions (Zolensky et al. 2008) both support the prominence of the pure Mg end-members. Olivine grains sized from 50 to 1100  $\mu\text{m}$  are present in the primitive Murchison meteorite (Olson & Grosman 1978). The average TOF-SIMS (time of flight secondary ion mass spectrometer) data for 67P aggregates are consistent with a mixture of olivine, pyroxene, and Fe-sulphide grains (Hilchenbach et al. 2016). A seeming lack of sulphur is due to a limitation in TOF-SIMS

analyses, which often use iron as a reference for Fe, Ni-sulphides, since quantitative sulphur measurements are difficult (Stephan et al. 2008). Fe-sulphides are consistent with the 67P IR spectra (Capaccioni et al. 2015). Fe-sulphide and Mg-olivine particles are predominant among the most primitive Solar system material. The 67P pebbles are assumed to be mixtures of: (1) Fe-sulphides of bulk density  $\rho_1 = 4600 \text{ kg m}^{-3}$  and abundance  $c_1$ ; (2) Mg, Fe-olivines and pyroxenes of bulk density  $\rho_2 = 3200 \text{ kg m}^{-3}$  and abundance  $c_2$ ; (3) hydrocarbons of bulk density  $\rho_3 = 1200 \text{ kg m}^{-3}$  and abundance  $c_3$ ; and (4) ices of bulk density  $\rho_4 = 917 \text{ kg m}^{-3}$  (Davidsson et al. 2016) and abundance  $c_4$ . The highest and lowest assumed bulk densities of the non-volatile component (Fe-sulphides and hydrocarbons) are consistent with the GIADA data (Fig. 1). The dust-to-ices mass ratio  $\delta$ , and the average bulk densities of the 67P nucleus  $\rho_N = 533 \text{ kg m}^{-3}$  (Pätzold et al. 2016) and of the dust  $\rho_D$  are

$$\delta = \frac{\rho_D}{c_4 \phi_1 \rho_4} \quad (1)$$

$$\rho_N = \phi_G (\rho_D + c_4 \phi_1 \rho_4) = (\delta + 1) c_4 \rho_4 \phi_G \phi_1 \quad (2)$$

$$\rho_D = \phi_P (c_1 \rho_1 + c_2 \rho_2 + c_3 \rho_3) = \frac{\delta \rho_N}{(\delta + 1) \phi_G}, \quad (3)$$

where  $\phi_G = 0.6$  (Onoda & Liniger 1990; Song et al. 2008) and  $\phi_P$  are the volume filling factors among the pebbles (related to macroporosity) and in the pebbles (related to microporosity), respectively. The high dust-to-ices ratio observed in 67P (Rotundi et al. 2015; Fulle et al. 2016) suggests that volatiles condense as thin compact layers of ice on the dust particles. We consider two possibilities: (1) ices are compact, with a volume filling factor  $\phi_1 = 1$ ; and (2) ices are porous,  $\phi_1 = \phi_P$ . In equation (3), the ices are replaced by voids after ice sublimation. Lower limits of  $\delta$  have been provided by coma observations of the gas and dust loss rates from the sunlit nucleus surface:  $\delta = 4 \pm 2$  on 2014 August–September (Rotundi et al. 2015); and  $5 < \delta < 100$  on 2015 August–September (Fulle et al. 2016), in pristine layers of the 67P nucleus exposed by the erosion of some metres during perihelion (Keller et al. 2015). The values of  $\delta$  and of the four volume abundances are fixed by equations (1)–(3), by the abundances normalization, and by a fifth equation fixing the  $c_2/c_1$  ratio. With  $\rho_D = 795 \text{ kg m}^{-3}$ , equation (3) provides  $\delta = 8.5$ ; the lower limit of  $\rho_D = 730 \text{ kg m}^{-3}$  provides  $\delta = 4.5$ ; the  $\rho_D$  upper limit is inconsistent with the random packing of pebbles (Onoda & Liniger 1990; Song et al. 2008) even for  $\delta > 100$ , and cannot be representative of the average non-volatile bulk density. Fig. 2 shows the volume abundances as functions of  $\phi_P$ . The abundances maintain a physical meaning only when all have positive values.

To constrain  $\phi_P$ , we consider the end-member cases of solar and CI-chondritic elemental abundances (Lodders 2003) in Fig. 2. For solar abundances, we fix the H/O ratio at the same ratio observed in CI-chondrites, implying that 99.97 per cent of hydrogen remained in the proto-planetary gas phase. We first consider the fraction of H and O atoms needed to obtain the ice abundances  $c_4$  provided by equation (2). Then we allocate half (Davidsson et al. 2016) of the remaining O atoms, all remaining H atoms, and all C and N atoms to hydrocarbons; the remaining O atoms and all Si, Na, Al, Ca, and Mg atoms are allocated to olivines and pyroxenes; and all Fe, Ni, and S atoms to Fe-sulphides. The silicates-to-sulphides ratio provides the  $c_2/c_1$  value. The results are independent of the actual content of CO and CO<sub>2</sub> in the ices, which is balanced by an exchange of C and H atoms between ices and hydrocarbons, to maintain the same  $c_4$  value.

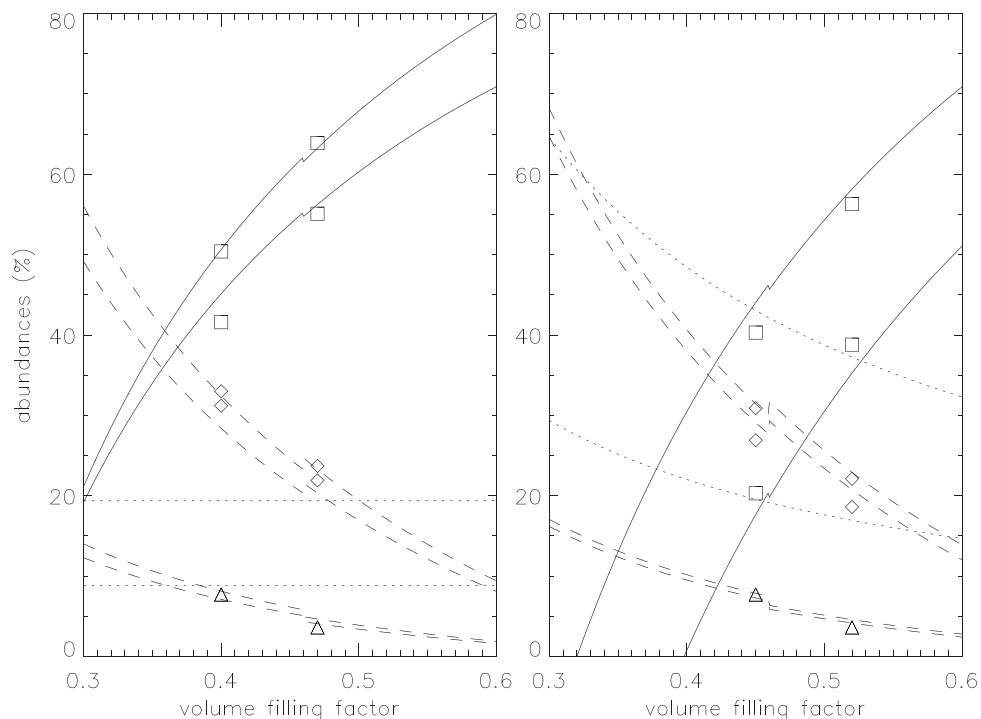


**Figure 2.** Volume abundances in planetesimals versus the volume filling factor in the pebbles  $\phi_P$  for compact (left-hand panel,  $\phi_1 = 1$ ) and porous ices (right-hand panel,  $\phi_1 = \phi_P$ ). The figure shows the predicted abundances of (1) Fe-sulphides,  $c_1$  (lower dashed lines), (2) Mg, Fe-olivines and pyroxenes,  $c_2$  (upper dashed lines), (3) hydrocarbons,  $c_3$  (continuous lines), and (4) ices,  $c_4$  (dotted lines; lower lines,  $\delta = 10$ ; upper lines,  $\delta = 4$ ). For all non-volatiles: upper lines,  $\delta = 10$ ; lower lines,  $\delta = 4$ ;  $c_2/c_1 = 4$  for  $\phi_P < 0.46$ ;  $c_2/c_1 = 5$  for  $\phi_P > 0.46$ ). They are compared to the abundances of hydrocarbons (squares), Mg, Fe-olivines and pyroxenes (diamonds) and Fe-sulphides (triangles) inferred from the solar ( $\phi_P > 0.46$ ) and CI-chondritic ( $\phi_P < 0.46$ ) chemical abundances (upper symbols,  $\delta = 10$ ; lower symbols,  $\delta = 4$ ).

In Fig. 2, we have assumed that silicates in 67P are Mg, Fe-olivines and pyroxenes. The matrix of the chondritic porous (CP) interplanetary dust particles (IDPs) contains spherical objects of glass with embedded metal and sulphide grains (GEMS; Bradley 1994). The bulk density of GEMS grains remains unknown but it is most likely between 2400 and 2800  $\text{kg m}^{-3}$ , matching most terrestrial glass densities. Some IDPs consist almost entirely of GEMS. Most of these IDPs are a mixture GEMS grains, Mg, Fe-silicates (olivine; pyroxene) and Fe(Ni)-sulphides, but GEMS tend to dominate in most CP IDPs (Rietmeijer 1998; Rietmeijer et al. 2002). The GEMS matrix is an amorphous magnesi silica glass with tiny metal and sulphide grains. More than 95 per cent of GEMS formed in the Solar system, the remainder coming from red giant branch or asymptotic giant branch stars or supernovae (Keller & Messenger 2011) or being interstellar dust (Rietmeijer 2009). The spherical GEMS grains range from 0.1 to  $\approx 1 \mu\text{m}$  in diameter (Rietmeijer 1998). When GEMS grains fuse together, they form larger amorphous silica grains (Rietmeijer 2011). In addition, other IDPs are amorphous Mg-Fe-Si grains without tiny metal and sulphide grains but containing Al and Ca. They are 0.5–1  $\mu\text{m}$  in size but when fused together they form amorphous Mg-Fe-Al-Ca-bearing silica grains that can be several microns in size (Rietmeijer 1998; Rietmeijer et al. 2002). In the Stardust samples of comet 81P/Wild 2, the glass bulk compositions match a GEMS composition but there is little evidence for spherical grains. Only two single spherical amorphous grains with embedded metal and sulphide grains have been reported (Leroux & Jacob 2013; Rietmeijer 2015), which could have been made during impact collection. To test the sensitivity of our model to the actual composition of 67P silicates in the dust aggregates

sampled by GIADA, in Fig. 3 we solve equations (1)–(3) assuming  $\rho_2 = 2600 \text{ kg m}^{-3}$ . We find that the only change into the solutions of equations (1)–(3) is a systematic shift of all the curves and data points of non-volatiles to slightly larger values of the volume filling factor  $\phi_P$ .

## 4 RESULTS AND CONCLUSIONS

The results in Figs 2 and 3 fit the predictions from equations (1)–(3) and indicate that the particles detected by GIADA have no bias in composition. Even more important, they are consistent with the primitive chemical abundances in our Solar system. Since 67P is a primordial rubble pile which has not been altered by collisions and heating (Davidsson et al. 2016), it follows that the Rosetta mission has really sampled the pebbles forming all planetesimals. The main difference between the two sets of abundances is a C-N-depletion in CI-chondrites versus solar abundances (Lodders 2003). Some Antarctic micrometeorites (Dartois et al. 2013) and stratospheric interplanetary dust particles (Rietmeijer & McKinnon 1985) are richer in C than provided by the solar abundances in Figs 2 and 3. The curves in Figs 2 and 3 related to a dust-to-ices mass ratio  $\delta = 8.5$  provide  $c_1 = (5 \pm 2)$  per cent,  $c_2 = (28 \pm 5)$  per cent,  $c_3 = (52 \pm 12)$  per cent, and  $c_4 = (15 \pm 6)$  per cent. A third class of GIADA particles [the GDS-only single particles (Fulle et al. 2015), which have a flux similar to GDS+IS ones] may be mostly composed of hydrocarbons, the most abundant in volume. Although most of 67P's volume is in the form of hydrocarbons, most of 67P's mass is in the form of sulphides and silicates. The average bulk density of

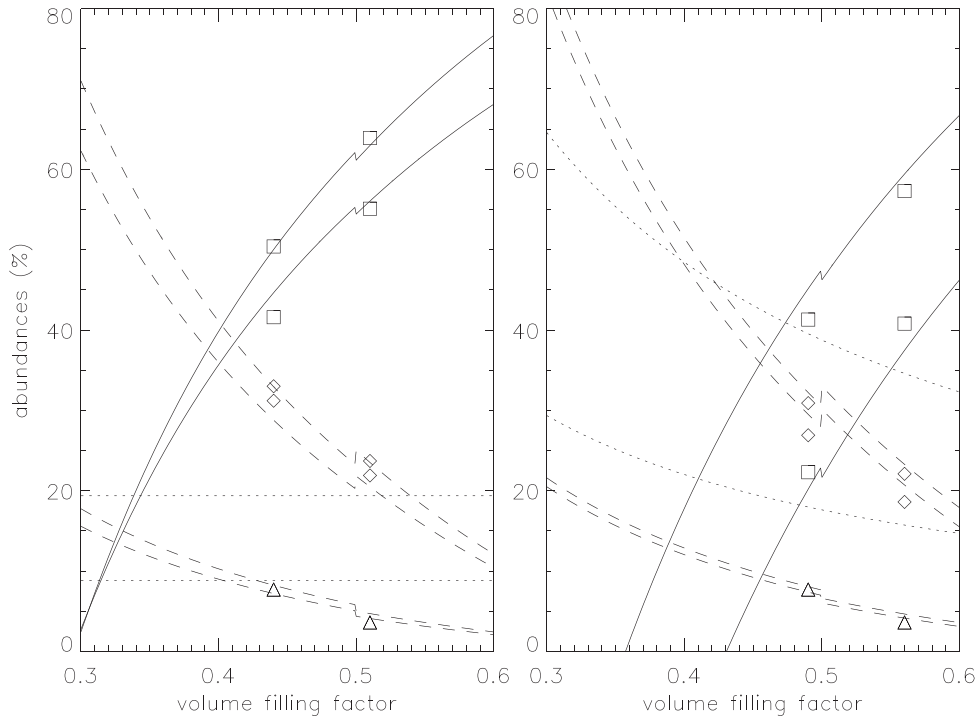


**Figure 3.** As Fig. 2, except that the upper dashed lines represent predicted abundances of amorphous silicates,  $c_2$ , with bulk density  $\rho_2 = 2600 \text{ kg m}^{-3}$  (rather than Mg, Fe-olivines and pyroxenes). Derived abundances are compared with solar chemical abundances ( $\phi_p > 0.5$ ) and chondritic abundances ( $\phi_p < 0.5$ ). See the text and Fig. 2 for details.

the compacted GIADA dust, i.e. of the non-volatile mixture without voids, is  $\rho_D/\phi_p = 1660_{-360}^{+2440} \text{ kg m}^{-3}$ .

The fits in Figs 2 and 3 constrain the pebble volume filling factor to  $\phi_p = 0.48 \pm 0.08$ , and the average porosity of the 67P nucleus (given by  $1 - \phi_G \phi_p$ ) to  $(71 \pm 8)$  per cent, i.e. lower than that inferred by RSI (Pätzold et al. 2016) and CONSERT (Kofman et al. 2015), which were computed neglecting the actual content of light hydrocarbons. The pebble microporosity is larger than the 67P nucleus macroporosity ( $\phi_p = 0.48$  versus  $\phi_G = 0.55$  or  $\phi_G = 0.65$  for random loose or close packing of spheres (Onoda & Liniger 1990; Song et al. 2008), respectively). This implies both a negligible compaction of the pebbles by gravity after gentle bouncing collisions, and bouncing velocities  $< 1 \text{ m s}^{-1}$  (Güttler et al. 2010) during the gravitational accretion of planetesimals, thus preserving some pristine fractals (67P's fluffy particles) in the voids among the compacted pebbles. The average ratio  $\phi_F/\phi_p \approx 10^{-3}$ , and the volume fraction of  $\approx 15$  per cent of fluffy parent particles (Fulle et al. 2015), imply that  $\approx 0.015$  per cent of the pristine fractals survived intact during the bouncing collisions compacting the pebbles. Both 67P's pebbles and fractals sample the primitive material which composed the proto-solar nebula.

## ACKNOWLEDGEMENTS

We warmly thank the referee, George Flynn, for his constructive suggestions that significantly helped to improve the manuscript. Rosetta is an ESA mission with contributions from its member states and NASA. Rosetta's Philae lander is provided by a consortium led by DLR, MPS, CNES, and ASI. We thank all the Rosetta instrument teams, the Rosetta Science Ground Segment at ESAC, the Rosetta Mission Operations Centre at ESOC and the Rosetta Project at ESTEC for their outstanding work enabling the science

return of the Rosetta Mission. GIADA was built by a consortium led by the Univ. Napoli Parthenope & INAF – Oss. Astr. Capodimonte, in collaboration with the Inst. de Astrofísica de Andalucía, ES, Selex-FI-IT and SENER-ES. GIADA is presently managed and operated by Ist. di Astrofísica e Planetologia Spaziali-INAF, IT. GIADA was funded and managed by the Agenzia Spaziale Italiana, IT, with the support of the Spanish Ministry of Education and Science MEC, ES. GIADA was developed from a PI proposal from the University of Kent; sci. & tech. contribution were provided by CISAS, IT, Lab. d'Astr. Spat., FR, and Institutions from UK, IT, FR, DE and USA. Science support was provided by NASA through the US Rosetta Project managed by the Jet Propulsion Laboratory/California Institute of Technology. We would like to thank Angioletta Coradini for her contribution as a GIADA Co-I. GIADA calibrated data will be available through ESA's PSA web site (<http://www.rssd.esa.int/index.php?project=PSA&page=index>). All data presented here are available on request prior to its archiving in the PSA. This research was supported by the Italian Space Agency (ASI) within the INAF-ASI agreements I/032/05/0 and I/024/12/0.

## REFERENCES

- Bradley J. P., 1994, *Science*, 265, 925
- Brownlee D. et al., 2006, *Science*, 314, 1711
- Burch J. L., Gombosi T., Clark G., Mokashi P., Goldstein R., 2015, *Geophys. Res. Lett.*, 42, 6575
- Capaccioni F. et al., 2016, *Science*, 347, aaa0628
- Dartois E. et al., 2013, *Icarus*, 224, 243
- Davidsson B. et al., 2016, *A&A*, 592, A63
- Della Corte V. et al., 2014, *J. Astron. Instrum.*, 3, 1350011
- Della Corte V. et al., 2015, *A&A*, 583, A13
- Della Corte V. et al., 2016, *Acta Astron.*, 126, 205

- Farinella P., Davies D. R., 1996, *Science*, 273, 938
- Ferrari M., Della Corte V., Rotundi A., Rietmeijer F. J. M., 2014, *Planet. Space Sci.*, 101, 53
- Fulle M. et al., 2015, *ApJ*, 802, L12
- Fulle M. et al., 2016, *ApJ*, 821, 19
- Güttler C., Blum J., Zsom A., Ormel C. W., Dullemond C. P., 2010, *A&A*, 513, A56
- Hilchenbach M. et al., 2016, *ApJ*, 816, L32
- Johansen A., Oishi J. S., Mac Low M.-M., Klahr H., Henning T., Youdin A., 2007, *Nature*, 448, 1022
- Keller L. P., Messenger S., 2011, *Geochim. Cosmochim. Acta*, 75, 5336
- Keller H. U. et al., 2015, *A&A*, 583, A34
- Kofman W. et al., 2015, *Science*, 349, aab0639
- Lambrechts M., Johansen A., 2012, *A&A*, 544, A32
- Leroux H., Jacob D., 2013, *Meteorit. Planet. Sci.*, 48, 1607
- Lodders K., 2003, *ApJ*, 591, 1220
- Olson D. W., Grosman X., 1978, *Earth Planet. Sci. Lett.*, 41, 111
- Onoda G., Liniger E. G., 1990, *Phys. Rev. Lett.*, 64, 2727
- Pätzold M. et al., 2016, *Nature*, 530, 63
- Rietmeijer F. J. M., 1998, in Papike J. J., ed., *Planetary Materials, Reviews in Mineralogy*, Vol. 36, Mineralogical Society of America, Chantilly, Virginia
- Rietmeijer F. J. M., 2002, *Chemie der Erde*, 62, 1
- Rietmeijer F. J. M., 2009, *ApJ*, 705, 791
- Rietmeijer F. J. M., 2011, *Icarus*, 211, 948
- Rietmeijer F. J. M., 2015, *Meteorit. Planet. Sci.*, 50, 1767
- Rietmeijer F. J. M., MacKinnon I. D. R., 1985, *Nature*, 315, 733
- Rietmeijer F. J. M., Hallenbeck S. L., Nuth J. A., Karner J. M., 2002, *Icarus*, 156, 269
- Rotundi A. et al., 2015, *Science*, 347, aaa3905
- Song C., Wang P., Makse H. A., 2008, *Nature*, 453, 629
- Stephan T. et al., 2008, *Meteorit. Planet. Sci.*, 43, 233
- Wahlberg Jansson K., Johansen A., 2014, *A&A*, 570, A47
- Youdin A., Goodman J., 2005, *ApJ*, 620, 459
- Zolensky M. E., Thomas K. L., 1995, *Geochim. Cosmochim. Acta*, 59, 4707
- Zolensky M. E. et al., 2008, *Meteorit. Planet. Sci.*, 43, 261
- Zsom A., Ormel C. W., Güttler C., Blum J., Dullemond C. P., 2010, *A&A*, 513, A57

This paper has been typeset from a  $\text{\TeX}/\text{\LaTeX}$  file prepared by the author.